Volume 1 | Number 1 | Jan 2013 | Pages 1–100

ChemComm

Chemical Communications
www.rsc.org/chemcomm

ROYAL SOCIETY OF CHEMISTRY

ROYAL SOCIETY OF CHEMISTRY

www.rsc.org/chemcomm

Table of Contents Abstract

Label-free Detection of Alzheimer's Disease through ADP3 Peptoid Recognizing Serum Amyloid-beta42 Peptide

Zijian Zhao,[a,1] Ling Zhu,[a,1,*] Xiangli Bu,[a] Huailei Ma,[a] Shu Yang,[a] Yanlian Yang,[a] and Zhiyuan Hu [a,*]

Surface plasmon resonance imaging in combination with ADP3 peptoid was used to identify Alzheimer's disease through detecting amyloid-beta42 in the serum.

ChemComm

COMMUNICATION

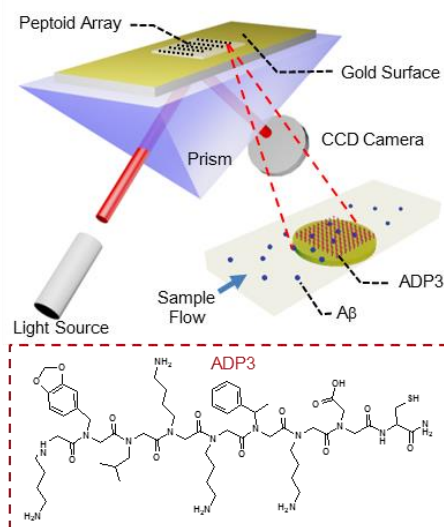# Label-free Detection of Alzheimer's Disease through ADP3 Peptoid Recognizing Serum Amyloid-beta42 Peptide

Zijian Zhao,[a,1] Ling Zhu,[a,1,*] Xiangli Bu,[a] Huailei Ma,[a] Shu Yang,[a] Yanlian Yang,[a] and Zhiyuan Hu[a,*]

The early diagnosis of Alzheimer's disease (AD) is challenging due to the lack of reliable method for detecting its biomarkers in the noninvasive biopsies. We used surface plasmon resonance imaging to identify AD based on detecting amyloid-beta42 in the serum by ADP3 peptoid.

Alzheimer's disease (AD), a neurodegenerative disorder characterized by progressive cognitive decline, is the most common form of dementia. Up to now, there is no effective treatment to stop or reverse the progression of AD. Early intervention is therefore crucial for the prognosis of this disease. However, the current diagnosis of AD is normally based on clinical symptoms, neuropsychological test, and neuroimaging. These observations may appear several years after the pathological changes.[1] The definite diagnosis can only be made by post-mortem autopsy confirming the existence of senile plaques and neurofibrillary tangles in the brain.[2] Early assessment methods are urgently required to improve the therapy of AD. For this purpose, assays have been developed to identify the biomarkers of AD.[3-5] Among these biomarkers amyloid beta (Aβ), total tau, and phosphorylated tau in cerebrospinal fluid (CSF) are widely accepted for the diagnosis of AD.[5,6] However, the invasive collecting procedure of CSF limits the application of these biomarkers. In this regard, blood-based biomarkers appear to be desired surrogates, and there is great need for the routine and reliable blood test to identify AD.

Amyloid-β, the main component of senile plaques, is a 39 to 43-residue peptide generated by cleavage of its precursor transmembrane protein amyloid precursor protein (APP).[7] Aβ is produced during normal cell metabolism and is present in body fluids including cerebrospinal fluid (CSF) and blood.[8,9] The deposition and aggregation of Aβ, especially the isoform Aβ42 in the brain is thought to be the initial step in the pathogenesis of AD.[10] Although numerous studies have shown reduced Aβ42 level in CSF correlated with AD[11] and the future development of AD in patients with mild cognitive impairment (MCI),[12,13] no agreement has been achieved about Aβ42 level in AD peripheral blood. Some reported elevated plasma Aβ42 level in AD[14] or incipient AD,[15] while others reported no change.[16,17] Despite these inconsistencies, vascular Aβ42 level has been shown to reflect the pathogenesis of AD,[18,19] and to be a valuable indicator for monitoring the effect of amyloid-targeting drugs.[20] The inconclusive results of the plasma Aβ42 level may be due to the analytical differences, or the complexity of the analyte. For example, the concentration of Aβ42 in serum is very

low (ten times lower than the one in CSF)[21,22] while the total serum proteins are abundant. Aβ42 may bind to serum proteins due to its hydrophobic properties.[14] These factors may affect the measured Aβ42 level by conventional immunoassays. Moreover, the labelling process of immunoassays is inconvenient and time-consuming.

Scheme 1. Schematic illustration of the method used to identify AD serum based on SPRi in combination with ADP3 peptoid array. ADP3 peptoids were fabricated on the gold-coated glass chip. The optical path from the laser passes through the coupling prism at a fixed angle of incidence, and the reflection is recorded by a charge-coupled device (CCD) camera. Upon injection of serum into the flow cell, Aβ42 in the serum is captured by ADP3, resulting in refractive index changes, and thus the reflection intensity changes detected by the CCD camera.

In this study, we used peptoid to identify AD serum utilizing surface plasmon resonance imaging (SPRi). Peptoids are unnatural synthetic N-substituted oligoglycines that have been used as antigen surrogates to identify and isolate target antibodies in the body fluids.[23,24] Gao et al. and Yam et al. developed a misfolded protein assay to detect misfolded protein aggregates including oligomeric Aβ42 from CSF based on aggregate specific reagent 1 (ASR1) peptoid that is conjugated to beads.[25,26] Reddy et al. performed a comparative screening of a peptoid library against AD and normal serum to search for antibody biomarkers and their relative capture

agents based on immunoassay method. They found that AD peptoids 3 (ADP3, Scheme 1) could identify AD through capturing immunoglobulin G (IgG) in the serum.[27] SPRi is a real-time, label-free and high-throughput sensor technique widely used to study biomolecular interactions occurring close to the SPR-active metal surface. In SPRi, the optical path from the laser passes through the coupling prism at a fixed angle of incidence, and the reflection intensity changes monitored by the CCD camera can be converted into the refractive index changes that result from molecular binding (Scheme 1).[28, 29] Here we combined ADP3 microarray and SPRi to develop a fast and label-free method for the diagnosis of AD.

Different concentrations of ADP3 ranging from 48 μM to 30 mM were immobilized onto the gold-coated glass chip, and serum samples from AD patients and age-matched non-demented control individuals were passed through the chip. At low concentration of ADP3 (< 1.2 mM, point I, II, III in Fig. 1a), the binding signals from AD and normal serum were low and similar (< 0.4 △ AU). When the concentration of ADP3 increased (> 5.9 mM, point IV and V in Fig. 1a), the binding signals from AD serum significantly increased compared to the ones from the normal serum, indicating that AD can be clearly segregated from the control at high concentration of ADP3 (Fig. 1a, S2).

To investigate what was captured by ADP3, we passed two antibodies individually through the chip after serum binding to ADP3: antibody against Aβ42, the widely reported AD biomarker, and antibody against human IgG, the highly present protein in human serum. We observed that the binding signals from anti-Aβ42 were significantly higher than the ones from anti-IgG in the AD group (Fig. 1b). This suggested that ADP3 selectively bound to Aβ42 in human serum, given that IgG existed in much higher abundance than Aβ42 in human serum. Furthermore, the binding signals from anti-Aβ42 were significantly higher in AD than the ones in the normal group (p < 0.01, Fig. 1b), indicating that more Aβ42 was captured by ADP3 in AD serum. The binding signal of anti-IgG was higher in normal control than in AD, but this difference was not significant (P > 0.05) due to the large data variance in the normal group (Fig. 1b). It has been reported before that AD patients might have a specific defect that causes lower level of IgG in the serum. However, the mechanism is still not clear.[30] These results implied that the higher SPRi response in AD serum compared to the normal one was from the binding of ADP3 to Aβ42. To explore this hypothesis, we checked the binding of pure Aβ42 to different concentrations of ADP3. The similar trend observed with AD serum was found with Aβ42 that at low concentration of ADP3 (< 0.79 mM, point I, II, III in Fig. 1c), the binding signals remained low, whereas at high concentration of ADP3 (> 2.4 mM, point IV, V, VI in Fig. 1c), the binding signals significantly increased (Fig. 1c). If we arranged the residues of ADP3 into a random order, which we referred to as scrambled ADP3, no binding was found with Aβ42 (S3). Moreover, the binding of ADP3 to human serum albumin (HSA) and immunoglobulin M (IgM), two of the most abundant proteins in serum, was negligible compared to the one to Aβ42 (Fig. 1d), further demonstrating the specificity of ADP3 to Aβ42. We further evaluated the binding affinity of ADP3 to Aβ42 through kinetic analysis of their interaction over a range of Aβ42 concentration. The resulting equilibrium dissociation constant (K_D value) was determined to be 1.64×10^{-9} M (data fitting using BIAevaluation 4.1 software (Biacore, Inc.), Fig. 1e), indicating the high binding affinity of ADP3 to Aβ42.

Taken together, these results indicated that ADP3 at high concentration could identify AD through binding to Aβ42 in the serum. The higher SPRi response in AD compared to the one in normal control was due to the higher level of Aβ42 in AD serum,

which is in agreement with the previously reported results.[14] We noticed that the binding signal of ADP3 to pure Aβ42 (∼0.5 △ AU) was lower than the one to AD serum (∼ 1.4 △ AU). This might be because that Aβ42 in the serum bound to plasma proteins[14] and the Aβ42-protein complexes therefore enhanced the SPRi response.
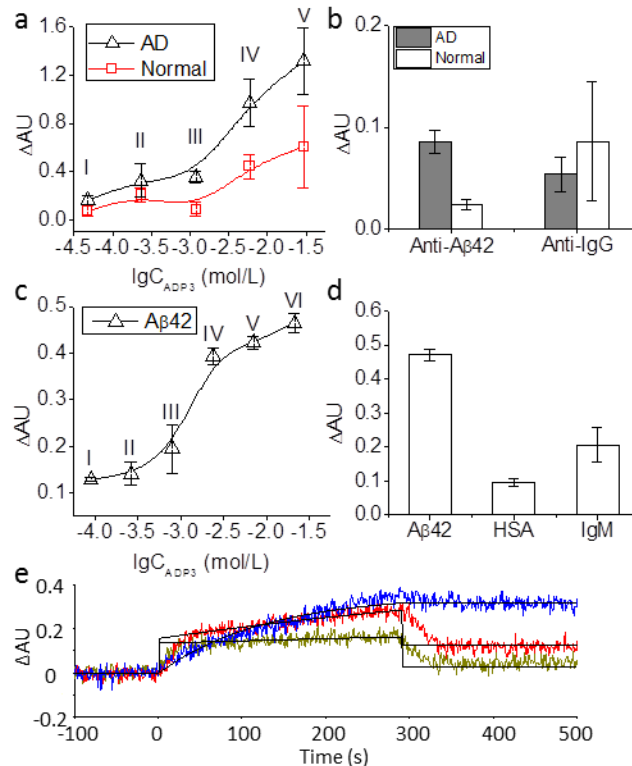

Fig. 1 High concentration of ADP3 could detect AD through specific binding to Aβ42 in the serum. (a) AD sera could be differentiated from the normal ones by high concentration of ADP3. The SPRi binding signals (changes of arbitrary unit, △ AU) are plotted as a function of the concentration of ADP3 immobilized on the chip. The black triangles represent data from AD patients, while the red squares represent data from normal individuals. (b) The binding signals of anti-Aβ42 and anti-IgG antibodies to the peptoid spot after serum binding to ADP3. (c) Pure Aβ42 binds to different concentrations of ADP3. Aβ42 was added at the concentration of 2.2 μM. (d) The binding signals from Aβ42, HSA, and IgM to ADP3 (29 mM). Error bars represent standard deviation (n=6 in (a) and (b), and n=3 in (c) and (d)). (e) Evaluation of the binding affinity of ADP3 to Aβ42. By analyzing the binding of ADP3 to different concentrations of Aβ42, the equilibrium dissociation constant (K_D) was determined. ADP3 was immobilized on the chip at the concentration of 5.9 mM. The green, red, and blue curves represent Aβ42 concentration of 0.089 μM, 0.44 μM, 2.2 μM, respectively. Data fitting was performed using BIAevaluation version 4.1 software (Biacore, Inc.).

To investigate the mechanism why ADP3 at high concentration could capture Aβ42 in the serum, we characterized the morphology of ADP3 adsorbed on the gold-coated SPRi chip at different concentrations by atomic force microscopy (AFM). At low ADP3 concentration (0.23 mM, corresponding to point II in Fig. 1a), no obvious peptoid adsorption was observed on the surface (Fig. 2a), though ADP3 molecules did adsorb on and cover the surface, which was

demonstrated by the materials scratched from the surface by the cantilever tip while increasing the scanning force (S4). At higher concentration of ADP3 (1.2 mM, corresponding to point III in Fig. 1a), nano-domains with the diameter of 150-250 nm and the height of ~15 nm appeared (marked with blue arrows in Fig. 2b). When the concentration of ADP3 increased to 5.9 mM (corresponding to point IV in Fig. 1a), the size of the domains increased to 300-500 nm (Fig. 2c). These results indicated that with increasing concentration, ADP3 could accumulate and self-assemble into flat domains, which might be responsible for Aβ42 binding. The immobilization of ADP3 on the gold surface was due to the covalent linkage through the cysteine group in the peptide. Considering the nanoscale height of these domains, we refer to them as nano-clusters. Notably, layers could be revealed in the nano-clusters (Fig. 2c), and the height of each layer was the multiple of ~4 nm (~4 nm, ~8 nm, ~16 nm, and ~20 nm) (Fig. 2d), indicating that the layers overlaid one on the other to form each nano-cluster.
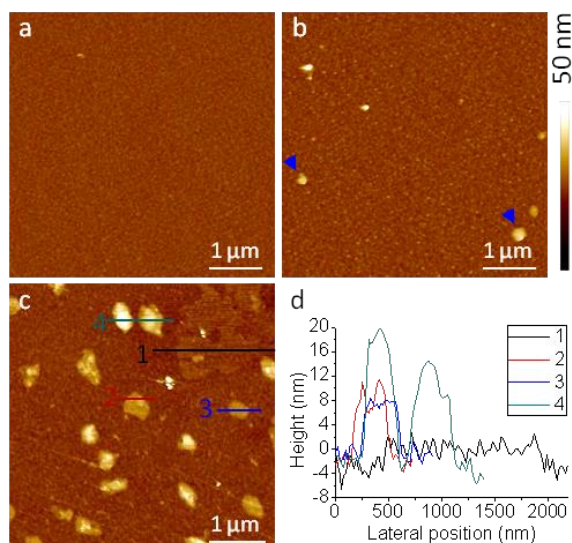

Fig. 2 AFM characterization of ADP3 adsorbed on the gold-coated SPRi chip at different concentrations. (a), (b), and (c) correspond to concentration II, III, and IV in Fig. 1a. (d) Height profile across the lines in (c), curve 1-4 correspond to line 1-4 in (c) respectively.

We then characterize the binding of Aβ42 to ADP3 nano-cluster. We chose the much smoother substrate mica to replace gold-coated glass in order to better reveal Aβ42. Unlike the immobilization on the gold surface that was through the covalent linkage, the immobilization here might be mainly through the electrostatic interaction between the positively charged side groups in the peptide and the negatively charged mica surface.[31] After being deposited onto the freshly cleaved mica, ADP3 formed a smooth nano-cluster with the height of ~1.7 nm covering the surface. Holes sized from 100 to 600 nm were observed (Fig. 3a). Zoom-in image further revealed small holes with the size ranging from 20 to 40 nm in the nano-cluster (Fig. 3b). Considering the height (~4 nm on gold, ~1.7 nm on mica) of the nano-clusters and the size (< 1.2 nm in height, ~4 nm in length) of the peptoid, it is most likely that the peptoid stayed upright on both surfaces as a "brush", but with different slopes (S5). These brush-like structures provided space for similar residues of ADP3 to be exposed, and might lead to the binding to Aβ42 in a similar way. In this respect, the nano-clusters on mica are good surrogates to the nano-clusters on the

gold surface to mimic the binding of Aβ42 to ADP3 peptoid. We deposited Aβ42 onto the nano-cluster, incubated for 5 mins and rinsed with water. We found that in the area where there were integrate ADP3 nano-clusters, the surface was covered by a layer of small dots, indicating the adsorption of Aβ42 (Fig. 3c). These dots were sized from 20 to 30 nm, in accordance
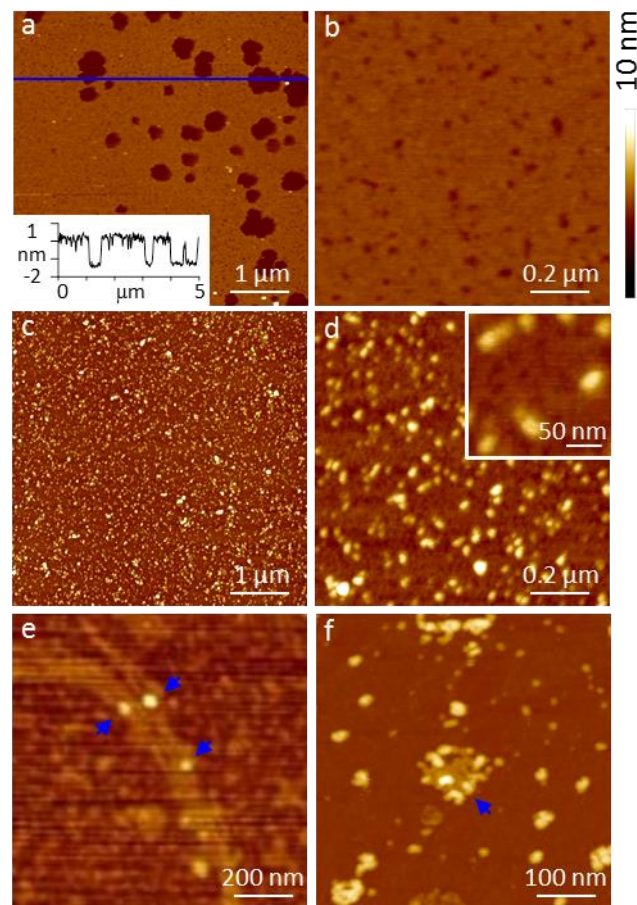

Fig. 3 AFM images showing the binding of Aβ42 to ADP3 nano-cluster. (a-b) ADP3 nano-clusters on mica. ADP3 was adsorbed on freshly cleaved mica at the concentration of 5.9 mM. Inset: Height profiles across the blue lines in (a). (c-d) Aβ42 adsorbed on integrate ADP3 nano-cluster at the concentration of 2.2 μM. (e-f) Aβ42 adsorbed on incomplete ADP3 nano-clusters. Blue arrows indicate the binding of Aβ42 to pieces of ADP3 nano-cluster.

with the size of Aβ42 oligomers previously reported.[32, 33] Zoom in image showed that the small holes were still visible underneath the layer of Aβ42 (Fig. 3d), indicating the presence of ADP3 nano-cluster underneath. These results suggested the binding of Aβ42 to ADP3 nano-cluster. For comparison, the same concentration of Aβ42 was deposited onto freshly cleaved mica. Significant difference was observed that without ADP3 nano-cluster, there was much less Aβ42 adsorbed on the surface (S6). Notably, in the area where the nano-clusters were incomplete, the adsorption of Aβ42 was only observed on nano-clusters, but not on the small holes where there was no nano-cluster (Fig. 3e, S7 a-e), further demonstrating the binding of Aβ42 to ADP3 nano-cluster. These results showed that the high-affinity of ADP3 to Aβ42 was associated with high concentration of ADP3 and the consequent appearance of

peptoid nano-clusters on the surface. This high-affinity may be due to the increased number of molecules on the surface, or the self-assembly structure. The binding affinity of the free ADP3 peptoid to Aβ42 was not determined and is unknown. However, the electrostatic interactions between the charged amines in ADP3 and the hydrophilic residues in Aβ42, and the hydrophobic interactions between the aromatic amines in ADP3 and the hydrophobic regions in Aβ42 may have effect on their interactions.[26, 34] The nano-clusters contribute to the high-affinity binding, but may not be the essential prerequisite that decide the binding. We noticed that the holes in the nano-cluster became smaller after binding to Aβ42. This might be because that the binding of Aβ42 changed ADP3 assembly and thus the morphology of the nano-cluster. This was verified in the area where there were big holes in the nano-clusters that after binding to Aβ42, some of the nano-clusters broke into pieces (S7 f). Zoom-in image showed that the remaining piece of ADP3 nano-cluster was surrounded by Aβ42 (marked with blue arrow in Fig. 3f), indicating that Aβ42 binding changed the morphology of ADP3 nano-cluster. We explained this as the binding strength between Aβ42 and ADP3 tore the nano-cluster and broke it into pieces, which further proved the high affinity of ADP3 to Aβ42.

In summary, we used ADP3 peptoid in combination with SPRi to identify AD serum. The identification was demonstrated to result from the binding of Aβ42 in AD serum to ADP3. This method provides an avenue toward the blood-based routine test for the early diagnosis of AD, and for monitoring the therapy effect of amyloid-targeting drugs.

Notes and references

a National Center for Nanoscience and Technology, No. 11, Beiyitiao Zhongguancun, Beijing, 100190, P.R. China

[1] Z. Z. and L. Z. contributed equally to this work.

* Corresponding authors: zhul@nanoctr.cn, huzy@nanoctr.cn

† Electronic Supplementary Information (ESI) available: [Experimental section, supplementary figures]. See DOI: 10.1039/c000000x/

1. D. A. Snowdon, S. J. Kemper, J. A. Mortimer, L. H. Greiner, D. R. Wekstein and W. R. Markesbery, *JAMA : the journal of the American Medical Association*, 1996, **275**, 528-532.
2. M. P. Mattson, *Nature*, 2004, **430**, 631-639.
3. A. Maddalena, A. Papassotiropoulos, B. Muller-Tillmanns, H. H. Jung, T. Hegi, R. M. Nitsch and C. Hock, *Archives of neurology*, 2003, **60**, 1202-1206.
4. D. G. Georganopoulou, L. Chang, J. M. Nam, C. S. Thaxton, E. J. Mufson, W. L. Klein and C. A. Mirkin, *Proceedings of the National Academy of Sciences of the United States of America*, 2005, **102**, 2273-2276.
5. K. Blennow, H. Hampel, M. Weiner and H. Zetterberg, *Nature reviews. Neurology*, 2010, **6**, 131-144.
6. L. Parnetti and D. Chiasserini, *Biomarkers in medicine*, 2011, **5**, 479-484.
7. D. J. Selkoe, *Trends in neurosciences*, 1993, **16**, 403-409.
8. C. Haass, M. G. Schlossmacher, A. Y. Hung, C. Vigo-Pelfrey, A. Mellon, B. L. Ostaszewski, I. Lieberburg, E. H. Koo, D. Schenk, D. B. Teplow and et al., *Nature*, 1992, **359**, 322-325.
9. P. Seubert, C. Vigo-Pelfrey, F. Esch, M. Lee, H. Dovey, D. Davis, S. Sinha, M. Schlossmacher, J. Whaley, C. Swindlehurst and et al., *Nature*, 1992, **359**, 325-327.
10. C. Haass and D. J. Selkoe, *Nature reviews. Molecular cell biology*, 2007, **8**, 101-112.
11. K. Blennow, *NeuroRx : the journal of the American Society for Experimental NeuroTherapeutics*, 2004, **1**, 213-225.
12. K. Blennow and H. Hampel, *Lancet neurology*, 2003, **2**, 605-613.
13. O. Hansson, H. Zetterberg, P. Buchhave, E. Londos, K. Blennow and L. Minthon, *Lancet neurology*, 2006, **5**, 228-234.
14. Y. M. Kuo, M. R. Emmerling, H. C. Lampert, S. R. Hempelman, T. A. Kokjohn, A. S. Woods, R. J. Cotter and A. E. Roher, *Biochemical and biophysical research communications*, 1999, **257**, 787-791.
15. R. Mayeux, M. X. Tang, D. M. Jacobs, J. Manly, K. Bell, C. Merchant, S. A. Small, Y. Stern, H. M. Wisniewski and P. D. Mehta, *Annals of neurology*, 1999, **46**, 412-416.
16. A. Tamaoka, T. Fukushima, N. Sawamura, K. Ishikawa, E. Oguni, Y. Komatsuzaki and S. Shoji, *Journal of the neurological sciences*, 1996, **141**, 65-68.
17. H. Vanderstichele, E. Van Kerschaver, C. Hesse, P. Davidsson, M. A. Buyse, N. Andreasen, L. Minthon, A. Wallin, K. Blennow and E. Vanmechelen, *Amyloid : the international journal of experimental and clinical investigation : the official journal of the International Society of Amyloidosis*, 2000, **7**, 245-258.
18. D. Scheuner, C. Eckman, M. Jensen, X. Song, M. Citron, N. Suzuki, T. D. Bird, J. Hardy, M. Hutton, W. Kukull, E. Larson, E. Levy-Lahad, M. Viitanen, E. Peskind, P. Poorkaj, G. Schellenberg, R. Tanzi, W. Wasco, L. Lannfelt, D. Selkoe and S. Younkin, *Nature medicine*, 1996, **2**, 864-870.
19. B. V. Zlokovic, *Trends in neurosciences*, 2005, **28**, 202-208.
20. E. R. Siemers, J. F. Quinn, J. Kaye, M. R. Farlow, A. Porsteinsson, P. Tariot, P. Zoulnouni, J. E. Galvin, D. M. Holtzman, D. S. Knopman, J. Satterwhite, C. Gonzales, R. A. Dean and P. C. May, *Neurology*, 2006, **66**, 602-604.
21. O. Hansson, H. Zetterberg, E. Vanmechelen, H. Vanderstichele, U. Andreasson, E. Londos, A. Wallin, L. Minthon and K. Blennow, *Neurobiology of aging*, 2010, **31**, 357-367.
22. C. Humpel, *Trends in biotechnology*, 2011, **29**, 26-32.
23. R. J. Simon, R. S. Kania, R. N. Zuckermann, V. D. Huebner, D. A. Jewell, S. Banville, S. Ng, L. Wang, S. Rosenberg, C. K. Marlowe and et al., *Proceedings of the National Academy of Sciences of the United States of America*, 1992, **89**, 9367-9371.
24. J. Sun and R. N. Zuckermann, *ACS nano*, 2013, **7**, 4715-4732.
25. C. M. Gao, A. Y. Yam, X. Wang, E. Magdangal, C. Salisbury, D. Peretz, R. N. Zuckermann, M. D. Connolly, O. Hansson, L. Minthon, H. Zetterberg, K. Blennow, J. P. Fedynyshyn and S. Allauzen, *PloS one*, 2010, **5**, e15725.
26. A. Y. Yam, X. Wang, C. M. Gao, M. D. Connolly, R. N. Zuckermann, T. Bleu, J. Hall, J. P. Fedynyshyn, S. Allauzen, D. Peretz and C. M. Salisbury, *Biochemistry*, 2011, **50**, 4322-4329.
27. M. M. Reddy, R. Wilson, J. Wilson, S. Connell, A. Gocke, L. Hynan, D. German and T. Kodadek, *Cell*, 2011, **144**, 132-142.
28. C. Lausted, Z. Hu, L. Hood and C. T. Campbell, *Combinatorial chemistry & high throughput screening*, 2009, **12**, 741-751.
29. S. Scarano, M. Mascini, A. P. Turner and M. Minunni, *Biosensors & bioelectronics*, 2010, **25**, 957-966.
30. M. E. Weksler, N. Relkin, R. Turkenich, S. LaRusse, L. Zhou and P. Szabo, *Experimental gerontology*, 2002, **37**, 943-948.
31. R. M. Pashley, *Journal of colloid and interface science*, 1981, **83**, 531-546.
32. P. Cizas, R. Budvytyte, R. Morkuniene, R. Moldovan, M. Broccio, M. Losche, G. Niaura, G. Valincius and V. Borutaite, *Archives of biochemistry and biophysics*, 2010, **496**, 84-92.
33. T. Ragaliauskas, M. Mickevicius, R. Budvytyte, G. Niaura, B. Carbonnier and G. Valincius, *Journal of colloid and interface science*, 2014, **425**, 159-167.
34. Y. Luo, S. Vali, S. Sun, X. Chen, X. Liang, T. Drozhzhina, E. Popugaeva and I. Bezprozvanny, *ACS chemical neuroscience*, 2013, **4**, 952-962.